Rev.Adv.Mater.Sci. 5 (2003) 239-244

SURFACE PROPERTIES OF NANOCRYSTALLINE ALLOYS CHARACTERISED BY MÖSSBAUER SPECTROMETRY

Marcel Miglierini

Department of Nuclear Physics and Technology, Slovak University of Technology, Ilkovičova 3, 812 19 Bratislava, Slovakia

Received: June 09, 2003

Abstract. FeMoXB (X = Cu, Au) NANOPERM-type nanocrystalline alloys are studied using Mössbauer spectrometry. Microstructure and magnetic arrangement is reviewed for the surface regions down to the depth of about 100 nm and for the bulk of the investigated specimens adopting the detection of conversion electrons and transmission geometry experiments, respectively. Nanocrystalline samples were prepared by a controlled annealing from originally amorphous precursors. Different temperatures of annealing chosen ensured varying amounts of nanocrystalline grains. Thus, the effects of mutual interactions among the crystallites and their impact on the surrounding amorphous retained phase were revealed. At the same time, consequences of composition changes on the microstructure and hyperfine interactions were inspected. In addition, samples with their surface being modified by laser irradiation are also discussed.

1. INTRODUCTION

Nanocrystalline alloys feature crystalline grains with the size of several nanometres that are embedded in amorphous residual phase. The usual way of their preparation comprises controlled annealing of amorphous precursors. Three main families of nanocrystalline alloys include FeNbCuSiB-type FINEMET [1], FeZrB(Cu)-type NANOPERM [2], and FeCoMBCu HITPERM [3] materials. Improved macroscopic magnetic properties of nanocrystalline alloys with respect to classical crystalline and/or amorphous ones [4] relate to their nanocrystalline microscopic character. Consequently, methods of microstructural analysis should be employed for clarification of the microstructure-to-macroscopic property relationship. Especially useful seems to be Mössbauer spectrometry which is capable of providing information both on structural arrangement and magnetic ordering.

NANOPERM-type alloys represent very suitable material for model studies because bcc-Fe, which emerges during the first crystallization process, is actually a calibration material for Mössbauer spectrometry. In this paper, the influence of composition as well as varying amounts of nanocrystallites on microstructure and magnetic arrangement of FeMoXB (X = Cu, Au) alloys is examined. The results for the bulk and for the surface of the investigated samples are discussed by the help of different techniques of Mössbauer effect measurements. Surface modification by laser treatment is also briefly discussed.

2. EXPERIMENTAL DETAILS

Amorphous precursors of $Fe_{80}Mo_7X_1B_{12}$ (X = Cu, Au) and $Fe_{76}Mo_8Cu_1B_{15}$ nominal composition were prepared by the method of planar flow casting in the form of ribbons (width of 3 and 6 mm, respectively, thickness of about 25 μm). Nanocrystalline samples were obtained by a heat treatment for 1 hour at temperatures spreading over the first crystallization peak as derived from differential scanning calorimetry.

Mössbauer spectra were recorded at room temperature in transmission geometry by a constant

Corresponding author: Marcel Miglierini, email: bruno@elf.stuba.sk

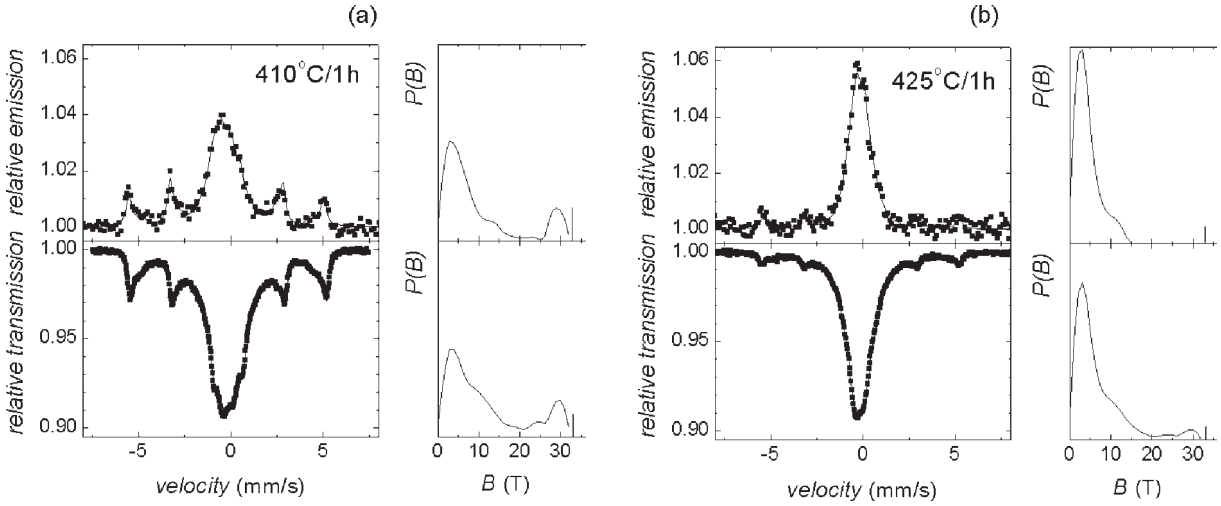

Fig. 1. CEMS (top panel) and TMS (bottom panel) spectra and corresponding distributions of hyperfine magnetic fields, *P(B)* (right) of the $Fe_{80}Mo_7X_1B_{12}$ alloy with low crystalline contents: X = Cu (a) and Au (b).

acceleration spectrometer with a ^{57}Co(Rh) source. Conversion electron Mössbauer spectrometry was applied to the dull side of the ribbons using a home-made apparatus [5]. Isomer shifts are quoted relative to a room temperature Mössbauer spectrum of bcc-Fe.

Laser treatments were performed with a XeCl excimer laser (Siemens XP2020) operating in a pulsed mode. Pulses of 55 ns duration, 308 nm wavelength were focused through a fly-eye homogenizer in order to obtain a uniform intensity distribution over a spot of 5x5 mm^2.

3. RESULTS AND DISCUSSION

Mössbauer effect experiments are usually performed in transmission geometry. By recording the intensity of the attenuated γ-ray beam from the source which traverses through the whole sample under investigation we are receiving information on structural properties and magnetic arrangement of the bulk of the latter. The incoming γ photons excite the sample which subsequently undergoes a de-excitation process. An excited nucleus can release its energy either by the emission of a fluorescent γ-ray having the same energy as the original one or via a non-radiative relaxation accompanied by an ejection of the so-called conversion electron. The vacant position left behind the released electron is occupied by electrons from the outer shells thus giving rise to the emission of characteristic X-rays. Different energies of the outgoing conversion electrons governed by their binding energy result in diverse escape depths of the order of several hundreds of nanometers. Conversion Electron Mössbauer Spectrometry (CEMS) makes use of this phenomenon thus enabling the very near surface states to be studied [6].

3.1. Low crystalline contents

Fig. 1 introduces room temperature spectra of the $Fe_{80}Mo_7X_1B_{12}$ (X = Cu, Au) nanocrystalline alloy with a low contents of nanograins taken by CEMS and transmission Mössbauer spectrometry (TMS) together with the corresponding distributions of hyperfine magnetic fields *P(B)*. Narrow lines represent contributions of the crystalline phase created during the heat treatment indicated. They are superimposed upon broadened features assigned to the retained amorphous phase. The thick vertical lines in the *P(B)* panels represent hyperfine field values of the crystalline phase identified as bcc Fe. Spectral parameters comprising average hyperfine field values of the amorphous residual <*B*> and crystalline B_{hf} phases, isomer shift d, relative contents A_{CR} and line intensity ratio A_{23} of the latter are listed in Table 1.

It should be noted that along with the spectral components representing the crystalline and amorphous phases, a third spectral component can be distinguished. It is characterised by a distribution of hyperfine fields in the vicinity of *B*-values of the crystalline phase and stems from atoms located on the surface of the grains.

Table 1. Average value of the hyperfine magnetic field of the residual amorphous phase <*B*>, and the crystalline phase B_{hf}, its isomer shift δ, relative contents A_{CR} and line intensity ration A_{23} as derived from TMS and CEMS of nanocrystalline $Fe_{80}Mo_7X_1B_{12}$ heat treated for 1 hour at the annealing temperature T_a and for the given composition *X*. The numbers in brackets give errors in the determination of the last digit.

X	T_a (°C)	*Method*	<*B*> (T)	B_{hf} (T)	δ (mm/s)	A_{CR} (%)	A_{23} –
Cu	410	TMS	8.40(5)	32.91(5)	-0.01(3)	17(3)	2.4
		CEMS	6.2(4)	32.7(1)	-0.08(10)	25(3)	4.0
Au	425	TMS	6.00(6)	33.04(5)	+0.01(4)	10(3)	2.6
		CEMS	4.3(2)	32.9(1)	+0.03(8)	13(3)	4.0
Cu	580	TMS	12.7(1)	32.79(5)	-0.01(3)	53(3)	1.0
		CEMS	8(1)	32.5(1)	+0.01(8)	71(3)	4.0
Au	620	TMS	11.2(7)	32.94(5)	-0.01(4)	59(3)	1.3
		CEMS	8(1)	32.9(1)	-0.00(8)	72(3)	4.0

The influence of composition on the progress of crystallization can be observed in Fig. 1. Copper forms crystallization centres and its replacement by Au, even though minute in amount, has a significant impact on the formation of nanograins. The surface crystallization in the X = Cu sample is already well developed at rather low annealing temperature of 410 °C whereas for X = Au it is only starting even at 425 °C.

From the point of view of the retained amorphous phase, the corresponding *P(B)* distributions exhibit higher probabilities at low hyperfine magnetic fields for X = Au. They indicate presence of atomic regions inside the amorphous residual phase which are paramagnetic. This is demonstrated by well pronounced central peak in Mössbauer spectra. These regions are supposed to be effectively enriched in Mo when Fe segregates into the nanocrystalline grains. Higher number of nearest Mo neighbours decreases the hyperfine fields of Fe atoms which is documented by low-field *B*-values in Fig. 1. This phenomenon is documented quantitatively in Table 1 by looking at the <*B*> values. Systematically lower <*B*>-values for CEMS spectra are due to higher crystalline contents A_{CR} which, on the other hand, makes Fe less abundant in the retained amorphous phase. Differences in <*B*> for X = Cu and Au are caused by deviations in chemical short range order documented by diversity of shapes of the accompanied *P(B)* distributions in Fig. 1.

Comparing the CEMS and TMS patterns for a given composition X one observes higher contribution of crystallites, i.e. more prominent progress of the crystallization process on the surface of the ribbon-shaped samples. On the other hand, intermediate hyperfine fields (≈ 20-25 T) are more pronounced in *P(B)* distributions corresponding to TMS rather than to the CEMS spectra for both X. This might be explained by a penetration of exchange ferromagnetic interactions among the grains by a way of local polarization of the retained amorphous phase [7].

3.2. High crystalline contents

Annealing at different temperatures alters the amount of nanocrystalline grains. As a result, magnetic exchange interactions among them exhibit distinct behaviour. An increased temperature of annealing, *i.e.* higher content of nanograins, is responsible for a growth of the magnetic ordering temperature of the retained amorphous phase. This phenomenon can be visualised by the help of Fig. 2. Room temperature Mössbauer spectra of $Fe_{80}Mo_7X_1B_{12}$ alloys with high contents of nanocrystallites exhibit variety of shapes due to deviations in the chemical and/or topological short-range order of the amorphous residual matrix caused by the segregation of Fe into the nanocrystals. Consequently, structural composition of the amorphous remainder is different as that of the original precursor (as-quenched amorphous alloy). This fact has an impact on the magnetic arrangement, too, which is demonstrated by obvious differences in the shape

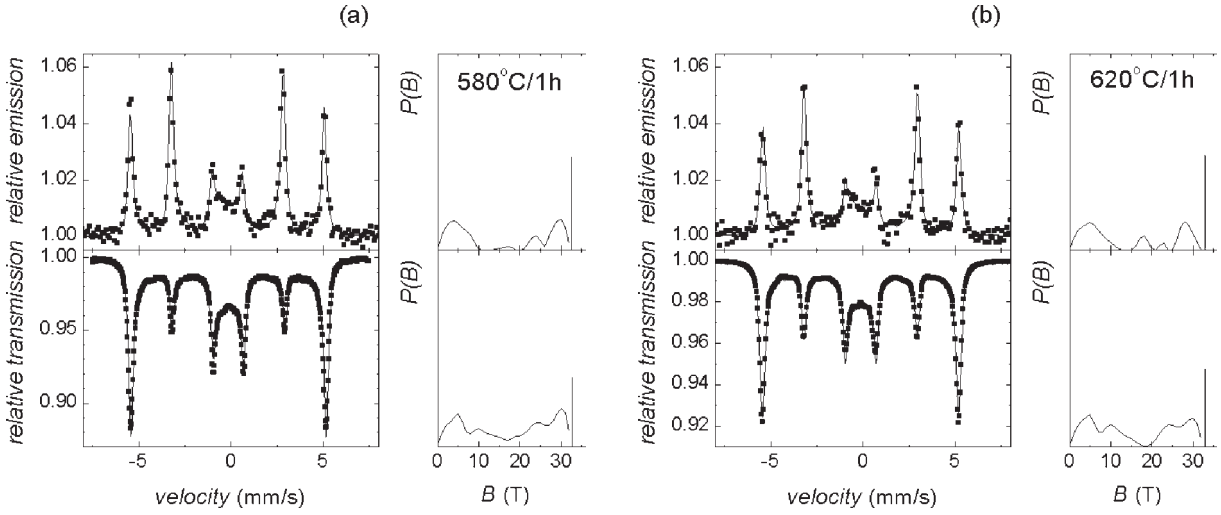

Fig. 2. CEMS (top panel) and TMS (bottom panel) spectra and corresponding distributions of hyperfine magnetic fields, *P(B)* (right) of the $Fe_{80}Mo_7X_1B_{12}$ alloy with high crystalline contents: X = Cu (a) and Au (b).

of the *P(B)* distributions with respect to those from Fig. 1. Especially low field *B*-values are suppressed on account of the intermediate and high *B*-values. Again, higher contribution of the former is better seen in TMS, *i.e.* in the bulk of the investigated nanocrystalline alloys. Spectral parameters are listed in Table 1. A notably higher amount of crystallites is revealed on the surface of the investigated samples.

Narrow lines in the Mössbauer spectra in Fig. 2 show well developed sextuplets characteristic for bcc Fe. For ^{57}Fe Mössbauer spectra, the ratio of the second (fifth) to the third (fourth) line intensity A_{23} is related to the direction of the net magnetic moment and varies between 4 and 0 for a parallel and a perpendicular orientation of the moment with respect to the plane of a ribbon-shaped sample, respectively. A random distribution of magnetic moment orientations gives the line intensity ratio of 2. The magnetic components in TMS and CEMS spectra in Fig. 2 show a tendency of magnetic moments to turn into the ribbon plane on the surface as indicated by the higher line-intensity ratio in CEMS. This is primarily caused by a creation of closure domains [8]. Distinctions in magnetic arrangement in the bulk and on the surface of the investigated samples are observed for both compositions (Table 1 and Fig. 2).

3.3. Surface modification

As-quenched $Fe_{76}Mo_8Cu_1B_{15}$ amorphous alloy exhibits close-to-room Curie temperature. Consequently, its Mössbauer spectrum consists of two contributions stemming from magnetic and non-magnetic regions of the resonant atoms. They are characterised by distributions of hyperfine magnetic fields *P(B)* and distributions of quadrupole splitting *P(QS)*, respectively. In fact, such spectra are very sensitive to external effects which can be effectively used for the study of subtle modifications of even amorphous structure [9]. We have used this alloy in nanocrystalline state obtained under various annealing conditions (different amount of nanograins) in order to inspect the effects of surface modification performed by laser irradiation.

Influence of laser treatment on nanocrystalline $Fe_{76}Mo_8Cu_1B_{15}$ with different contents of crystalline phase is documented by Table 2. Average value of the hyperfine magnetic field of the residual amorphous phase <*B*>, its relative content A_B, and the relative content of non-magnetic amorphous regions A_{QS} are listed for untreated nanocrystalline samples and for the samples treated with one laser pulse with the energy density H = 0.2 Jcm^{-2} in nitrogen atmosphere. The nanocrystalline samples were prepared by annealing for one hour at the annealing temperature T_a = 490, 510, and 600 °C giving rise to 26, 39, and 60% of crystalline phase before laser irradiation, respectively.

CEMS Mössbauer spectra of the 600 °C annealed $Fe_{76}Mo_8Cu_1B_{15}$ alloy after laser treatment with one pulse with the indicated energy densities are shown in Fig. 3. Laser treatment was performed in the atmosphere of nitrogen. Corresponding TMS

Table 2. Average value of the hyperfine magnetic field of the residual amorphous phase <*B*>, its relative content A_B, and the relative content of non-magnetic amorphous regions A_{QS} derived from CEMS of nanocrystalline $Fe_{76}Mo_8Cu_1B_{15}$ heat treated for 1 hour at the annealing temperature T_a and irradiated with the energy density of the laser *H*. The numbers in brackets give errors in the determination of the last digit.

T_a (°C)	H (Jcm^{-2})	<*B*> (T)	A_B (%)	A_{QS} (%)
490	0	12.7(5)	22(3)	52(3)
	0.2	9.2(6)	50(3)	20(3)
510	0	14.4(8)	21(3)	40(3)
	0.2	12.0(7)	29(3)	28(3)
600	0	14.8(6)	17(3)	23(3)
	0.2	14.6(7)	18(3)	22(3)

spectra do not show any qualitative changes with increasing energy and that is why they are not provided on a separate figure.

A gradual decrease of the crystalline component is observed on the surface as a function of the laser's energy density. Surface melting caused by the laser beam and subsequent rapid quenching due to the thermal contact with neighbouring regions of the sample's material have lead to complete re-amorphization after the irradiation with H = 0.75 J· cm^{-2}. As a result, the corresponding Mössbauer spectrum shows only broadened central doublet which was fitted with one distribution on quadrupole splitting values. So, the magnetic regions of the retained amorphous phase (comprising in this case 100% of the surface) have vanished entirely, too.

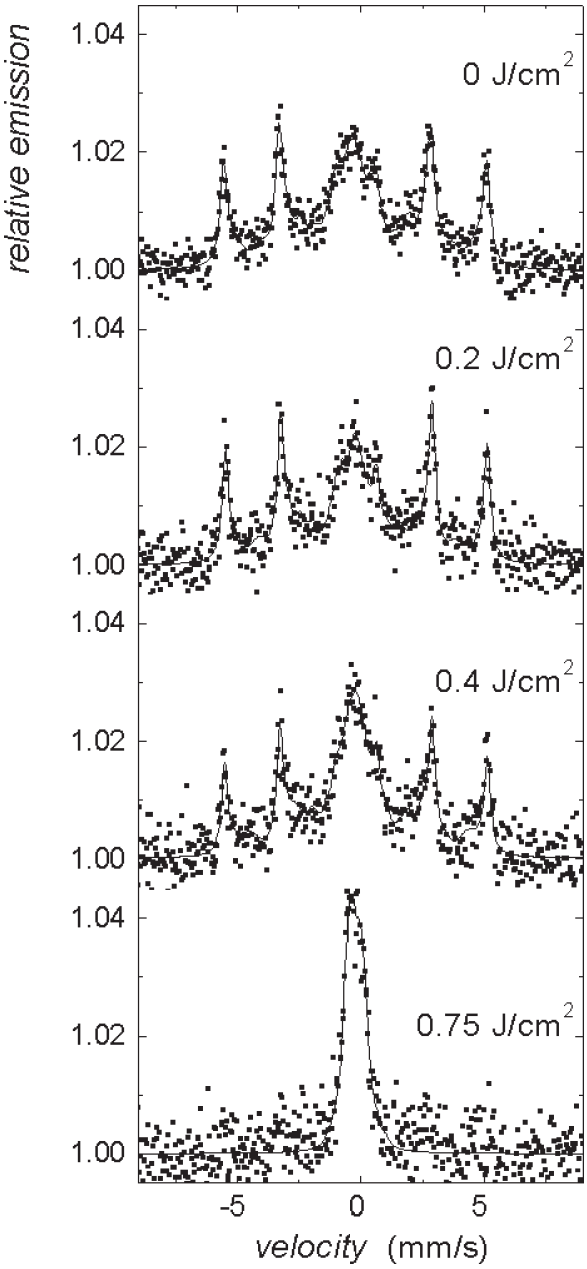

Fig. 3. CEMS spectra of the nanocrystalline $Fe_{76}Mo_8Cu_1B_{15}$ alloy after laser treatments with one pulse with the indicated energy density.

4. CONCLUSIONS

NANOPERM-type $Fe_{80}Mo_7X_1B_{12}$ (X = Cu, Au) alloys exhibit compositional dependent behaviour. During the first stages of crystallization, formation of nanograins is more pronounced for X = Cu than for Au-containing alloys. Mössbauer spectrometry has revealed the appearance of magnetic interactions even via the paramagnetic amorphous phase. They are due to magnetic exchange among bcc Fe nanograins created during the annealing. Differences in hyperfine interactions between surface regions and bulk of the alloys inspected by conversion electron Mössbauer spectrometry and by transmission Mössbauer spectrometry, respectively, are displayed by the help of distributions of hyperfine fields. The impact of which element is present on the microstructure and magnetic arrangement is crucial during the commencement of the crystallization but it cannot be discerned for high crystalline contents. In the latter, however, deviations in the orientation of the net magnetic moments on the surface and in the bulk are more apparent.

Nanocrystalline $Fe_{76}Mo_8Cu_1B_{15}$ alloy has exhibited surface re-amorphization after laser treatment with sufficiently high energy density of the laser (0.75 Jcm^{-2}). Lower energy of laser irradiation has affected only the relative ratio of the crystalline-to-amorphous phase contents of the surface regions. Practically no changes were observed in the bulk. It should be noted, however, that the above mentioned effects were obtained after the laser treatment with a single pulse per irradiation spot.

ACKNOWLEDGEMENT

Amorphous precursors were prepared by B. Idzikowski (Poznań) and D. Janičkovič (Bratislava). Surface modifications were performed by the courtesy of P. Schaaf (Göttingen) within the frame of the DAAD project No. 8/2003. This work is supported by the grant 1/8305/01.

REFERENCES

[1] Y. Yoshizawa, S. Oguma and K. Yamauchi // *J. Appl. Phys*. **64** (1988) 6044.

[2] K. Suzuki, N. Kataoka, A. Inoue, A. Makino and T. Masumoto // *Mater. Trans*. *JIM* **31** (1990) 734.

[3] A.M. Willard, E.D. Laughlin, M.E. McHenry, D. Thoma, K. Sickafus, J.O. Cross and V.G. Harris // *J. Appl. Phys.* **84** (1998) 6773.

[4] A. Makino, A. Inoue and T. Masumoto // *Mater. Trans. JIM* **36** (1995) 924.

[5] M. Seberíni and J. Degmová // *Czech. J. Phys.* **47** (1997) 559.

[6] J. R. Gancedo, M. Gracia and J. F. Marco, In: Material Research in Atomic Scale by Mössbauer Spectroscopy, ed. by M. Mashlan, M. Miglierini and P. Schaaf (Kluwer Academic Publishers, Dordrecht, 2003) p.41.

[7] I. Navarro, M. Ortuńo and A. Hernando // *Phys. Rev.* **B 53** (1996) 11656.

[8] U. Gonser and P. Schaaf // *Fresenius J. Anal. Chem.* **341 (**1991) 131.

[9] M. Miglierini, P. Schaaf, I. Škorvánek, D. Janičkovič, E. Carpene and S. Wagner // *J. Phys.: Condens. Matter.* **13** (2001) 10359.